Available online at www.sciencedirect.com
SCIENCE DIRECT®

Journal of the European Ceramic Society 23 (2003) 1427–1434
www.elsevier.com/locate/jeurceramsoc

Internal stresses in $BaTiO_3$/Ni MLCCs

Young-Il Shin[a], Kyung-Moo Kang[a], Yeon-Gil Jung[a], Jeong-Gu Yeo[b], Sang-Gyu Lee[b], Ungyu Paik[b,*]

[a]*Department of Ceramic Science and Engineering, Changwon National University, Changwon, Kyungnam 641-773, South Korea*
[b]*Department of Ceramic Engineering, Hanyang University, Seoul 133-791, South Korea*

Received 21 May 2002; received in revised form 16 September 2002; accepted 28 September 2002

Abstract

The internal stresses in $BaTiO_3$ based multilayer ceramic capacitors (MLCCs), showing Y5V characteristics, were estimated with a sharp indentation method using a micro-indenter. The influence of the direction to electrode on the internal stresses, especially residual stresses, was investigated at the three planes (*x*, *y*, and *z* planes), including the effect of the distance from the electrode on hardness. Hardness is constant to a special distance from the electrode, depending on the plane, and modestly decreases above that distance. The internal stresses at the planes parallel to the electrode, *x* and *y* planes, indicate the compressive and tensile stresses in the directions parallel (*x* and *y* directions at *x* and *y* planes, respectively) and perpendicular (*z* direction) to the electrode, respectively. The internal stresses at the plane perpendicular to the electrode, *z* plane, are compressive in both directions. The extrinsic stress induced by the fabrication process is tensile, which is much severer than the intrinsic stress by the material constants. The internal stresses created on MLCCs are dependent on the plane with the lamination and the direction to the electrode, parallel and perpendicular directions. Crack formation and damage mode related to the internal stresses are also discussed.

Keywords: $BaTiO_3$; Capacitors; Defects; Internal stresses

1. Introduction

Multilayer ceramic capacitors (MLCCs) continue to be one of the most widely used and most important passive components in the circuitry of electronic products.[1,2] MLCCs are subjected to manufacturing or service thermomechanical and residual stresses which, if severe enough, will cause mechanical failure and perhaps subsequent loss of electrical function. Increasing the number and reducing the thickness of the active layer for high capacitance in MLCCs, can cause problems due to the difference of density and thermal expansion coefficient between the inner regions with electrode and the outside regions (margins) without electrode, resulting in structural defects and crooked shapes. The delamination and cracks, becoming multilamination in MLCCs, can also be due to internal stresses and created during the firing process.

Therefore, the reliability and the lifetime of MLCCs are dependent on removing and/or controlling internal stresses and structural defects as the number and the thickness of the active layer increase and decrease, respectively. Furthermore, these internal stresses can cause failure of capacitors because a tensile stress of 30–50 MPa is generated during end-termination and soldering.[3] Franken and Maier reported that a compressive residual stress between approximately −40 and −90 MPa has been found near the termination in MLCCs of different sizes.[4] Wereszczak et al. reported that the residual stresses, as calculated by finite element analysis (FEA), in the margins of multilayer capacitors (MLCs) are dependent on the direction, with a compressive stress of 240–277 MPa in the direction parallel to the electrode and a tensile stress of 230 MPa in the direction perpendicular to the electrode.[5]

The estimation and the understanding of the internal stresses induced on MLCCs are essential for improving the reliability and the lifetime of MLCCs. For the measurement of the internal stresses (residual stresses), the X-ray diffraction $\sin^2\psi$ method,[6,7] the conventional

* Corresponding author. Tel.: +82-2-2290-0502; fax: +82-2-2281-0502.
E-mail address: upaik@hanyang.ac.kr (U. Paik).

0955-2219/02/$ - see front matter
PII: S0955-2219(02)00346-1

beam-bending technique,[4,8,9] and the sharp indentation method including nano-indentation,[10–14] are available. Among the various techniques available, the sharp indentation method using a micro-indenter was used in this study.

In this paper, the influences of the direction with respect to lamination and the distance from electrode on hardness, crack formation, and internal stresses have been investigated with $BaTiO_3$ based Ni–MLCCs, showing Y5V characteristics. In addition, the relationship between damage modes and internal stresses has been discussed.

2. Experimental procedure

2.1. Materials and preparation

The MLCCs samples used in this experiment were commercial products showing Y5V characteristics. The dimensions of MLCCs specimens were 3×2×1.6 mm with 150 active layers including the housing regions (margins) of ≈250 μm. The thickness of dielectric and electrode layers was ≈8 and ≈2 μm, respectively. For measuring fracture toughness of the dielectric layer only, the standard specimen—that is, bulk specimen without electrode—was prepared by the same conditions with the MLCCs after laminating the green sheets only.

The specimens to be used for indentation were prepared by grinding to a 10 μm finish and subsequently polished to 1 μm. To remove the residual stresses due to grinding and polishing, the specimens were also polished with SiO_2 colloid sol of 10 nm. Selected polished surfaces were gold-coated to reveal surface condition and examined by optical microscopy (Epiphon, Nickon, Japan) and scanning electron microscopy (SEM, S2700, Hitachi, Japan).

2.2. Hardness and residual stress measurement

In this present study, the hardness and the residual stress of "margins" in the MLCCs were measured by considering the effects of the direction with respect to the lamination and the distance from the electrode. To eliminate the effect of end-termination, the measurement was carried out with only chips after post-annealing at the temperature of 950 °C—that is, MLCCs without end-termination. All indentations were made with a micro-hardness tester (Mitutoyo, AVK-C2, Japan) using a diamond Vickers shaped indentor. Hardness in the different planes, the x–y plane (hereafter x plane, as shown in Fig. 1) and the y-z planes (hereafter y and z planes parallel and perpendicular to the electrode, respectively, as shown in Fig. 1), was measured after indentation with a load of 0.25 N for 15 s, as a function of the direction (parallel and perpendicular), and the distance from the electrode, shifting the measuring position from the electrode to the surface in each plane. The internal stresses were determined by measuring the crack length after indentation with the load range from 0.25 to 1 N, in the same manner as for hardness. The cone diameter and crack length were measured using optical microscopy and SEM. The residual stresses were determined by the following expression:

$$K'_{IC} = K^{o}_{IC} + 2\sigma_R(C/\pi)^{1/2},$$

where K_{IC}' and K^{o}_{IC} are the fracture toughness values with and without residual stresses, C is the crack length, and σ_R is the residual stresses induced on the MLCCs. K^{o}_{IC} is determined as 0.85 MPa $m^{1/2}$ because K^{o}_{IC} in the bulk specimen shows the range of 0.74∼0.95 MPa $m^{1/2}$, depending on the direction with respect to the lamination, and literature indicates 0.85 MPa $m^{1/2}$ as the value of K^{o}_{IC}.[3]

3. Results and discussion

The hardness, H, obtained from indentation versus the distance from the electrode is plotted in Fig. 2. The hardness in the x plane is essentially constant in a range of 10±1.6 GPa to a distance of ≈70 μm, after which it slightly decreases to about 8.2±1.6 GPa. In the y plane, the hardness displays a similar trend as for the x plane, showing a range of 9.7±1.2 GPa to a distance of ≈45 μm and decreasing to about 6.8±1.0 GPa at the far away regions from the electrode. The hardness in the z plane is a little higher than those of the other two planes, showing a range of 11±1.2 GPa to ≈90 μm and 8.3±1.5 GPa at the far position. However, the tendencies are similar to each other. The decrease of hardness at the far position from the electrode, near the surface, will be related to the residual stresses induced on the interface between dielectric material ($BaTiO_3$) and Ni electrode layers. The residual compressive stress formed during cooling from the post-annealing temperature of 950 °C due to thermal expansion mismatch affects hardness as well as Young's modulus.[15,16]

Fig. 3 shows the difference in crack length between the parallel (hereafter x direction at the x plane and y direction at the y and z planes) and perpendicular (hereafter z direction at all plane) directions to the electrode. The crack length was measured by optical microscopy and/or SEM after Vickers indentation on each plane. The difference and scatter between the crack lengths increases with increasing indentation load and the distance from the electrode. For the x and y planes, the crack length in the x and y directions is larger than that in the z direction, indicating that relative compressive and tensile stresses are created in the x and y directions, and in the z direction, respectively. However, for

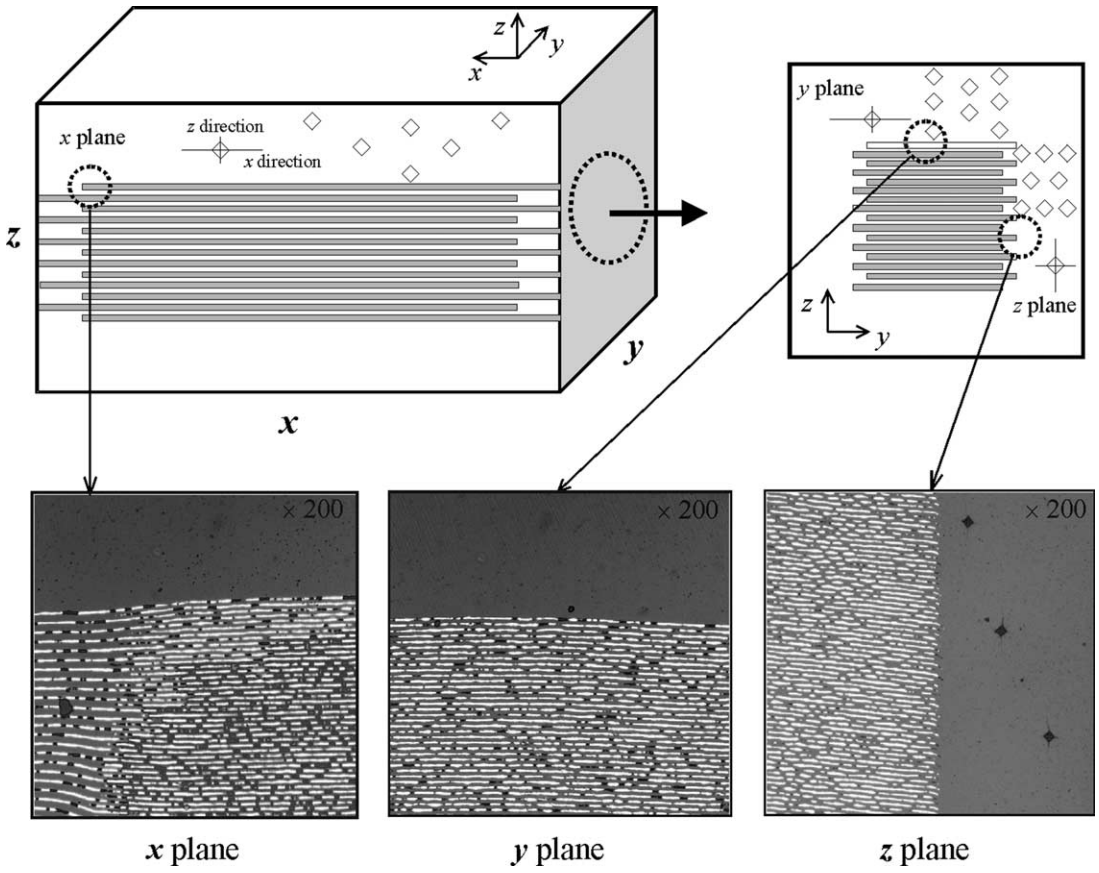

Fig. 1. Schematic diagram of indentation site for measurement of hardness and internal stresses and optical micrographs of each surface in the MLCCs.

the z plane, the crack length is not much different from each other—y and z directions, which means that internal stresses are not dependent on the direction in the z plane, compared to the other planes.

It is evident from Fig. 4 that the relative tensile and compressive stresses induced in the x and y directions at the x and y planes, respectively, result in a crack length that is modestly increased as the distance from the electrode is increased, indicating that the residual stress due to thermal expansion mismatch between the dielectric and electrode layers affects the crack length. However, the z plane does not show the dependence of the direction and distance. Usually, the shrinkage ratio in MLCCs depends on the direction and the number of the active layer, showing smaller shrinkage in the thickness direction (z direction) rather than the length and width directions (x and y directions) with an increase of the active layer. Therefore, the crack length at the z plane can be balanced with the direction and distance.

The residual stresses, σ_R, induced in each direction of planes are shown in Fig. 5. A compressive stress of -53 ± 10 and -78 ± 8 MPa is generated in the x and y directions at the x and y planes, and a tensile stress of 36 ± 43 and 3 ± 43 MPa in the z direction at the x and y planes, respectively. The tensile stress created in the z direction at the x and y plane is relatively small, considering the scatter. At the z plane, a compressive stress of -76 ± 30 and -100 ± 19 MPa is induced in the y and z direction, independent of the direction. As a result, it is found that the internal stresses at the x and y planes of MLCCs are compressive and tensile in the directions parallel and perpendicular to the electrode, respectively, and are also dependent on the laminated direction. However, the internal stress at the z plane is compressive stress only, even the absolute value is dependent on the direction.

For the formation of internal stresses on the margins of MLCCs, two possible reasons are under consideration. The internal stresses in MLCCs may be induced from the contributions of the thermal/intrinsic stress and extrinsic (due to the fabrication process) stress components: (1) mismatch of material constants such as thermal expansion coefficient, elastic modulus, Poisson's ratio, between dielectric and electrode layers; (2) microstructural defects introduced by the laminating, burnout and sintering processes. In order to separate these contributions in the internal stresses, the thermal stress is calculated using the following expression:

$$\sigma_{\text{thermal}} = \Delta\alpha\cdot\Delta T\cdot((E_d\cdot E_e)/(E_d\cdot(1\text{-}\nu_e) + E_e\cdot(1\text{-}\nu_d)),$$

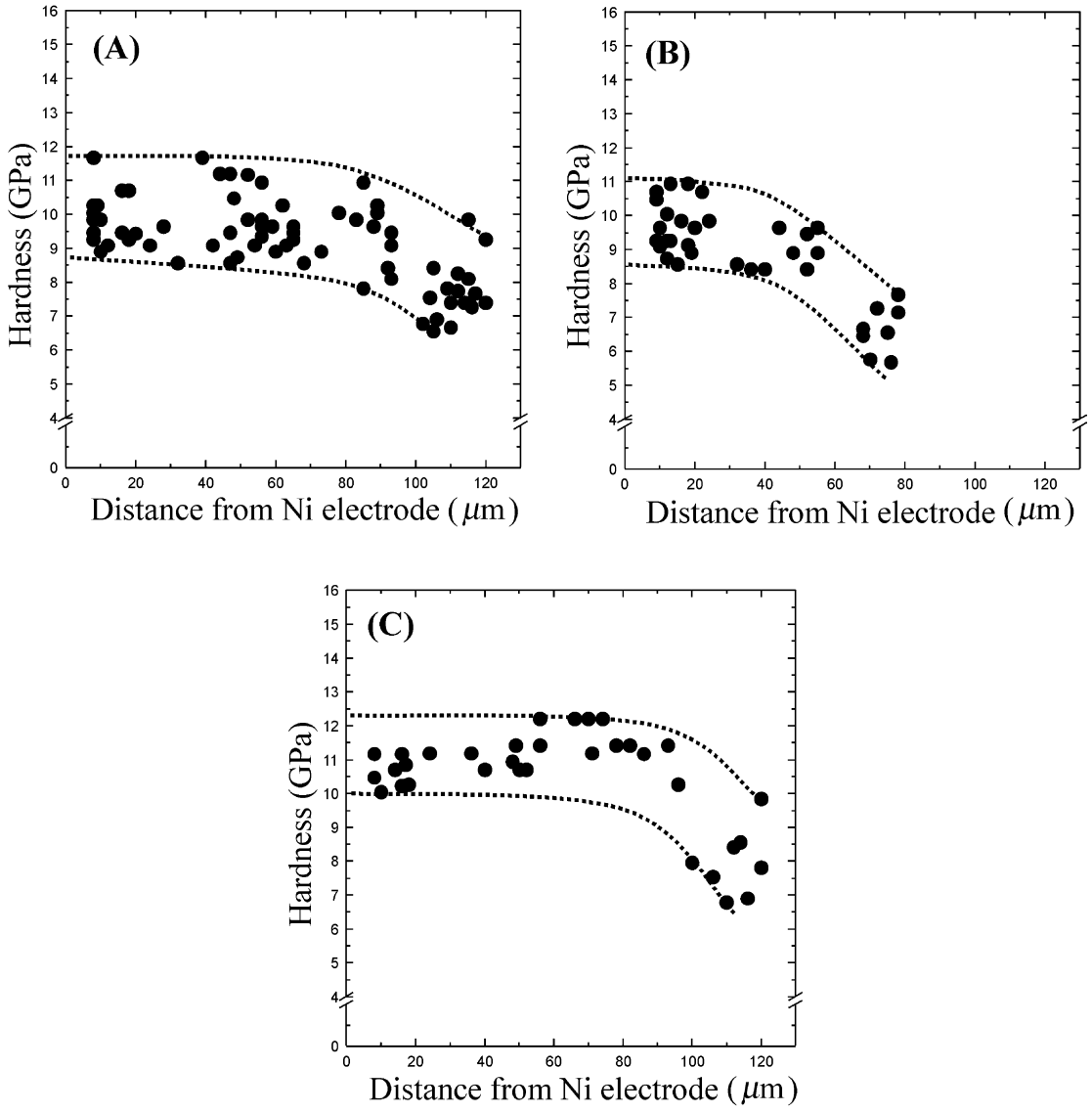

Fig. 2. Hardness versus distance from electrode with indentation load $P=0.25$ N: (A) x plane, (B) y plane, and (C) z plane.

where $E_{d,e}$ and $\nu_{d,e}$ are the elastic modulus and Poisson ratio of the dielectric and electrode layers, respectively. $\Delta\alpha$ is the difference in thermal expansion coefficient between the dielectric and electrode layers, and ΔT is the difference in temperature between the post-annealing and room temperatures. The dielectric formulation showing Y5V characteristics is $Ba_{0.95}Ca_{0.05}Ti_{0.825}Zr_{0.175}$ (Kyorix Co., Japan) + various metal oxide additives (such as Y_2O_3, MnO_2, SiO_2; High Purity Chem. Ltd., Japan). For this work, materials have been taken as $BaTiO_3$ and Ni because the total amounts of additives are less than 1 wt.% of the formulation. The thermal stresses are calculated using the following values; [17–19] $\alpha_{BT}=9.5\sim11.5\times10^{-6}\ ^{\circ}C^{-1}$, $\alpha_{Ni}=13.3\times10^{-6}\ ^{\circ}C^{-1}$, and $E_{BT}=125$ GPa, $E_{Ni}=200$ GPa, and $\nu_{BT}=0.25$, $\nu_{Ni}=0.31$, and $\Delta T=925\ ^{\circ}C$.

Fig. 6 shows the relative residual stresses calculated from the crack length after indentation with a load of 0.5 N, including the thermal stress. The thermal stress calculated above the equation is a compressive stress of -274 ± 97 MPa. However, the residual stress measured in the x direction at the x plane and the y direction at the y plane is compressive, showing -3 ± 65 and -21 ± 18 MPa, respectively. The compressive stress modestly increases with an increase of the distance from the electrode. The residual stress in the z direction is tensile, 160 ± 136 MPa at the x plane and 165 ± 124 MPa at the y plane, with a large scattering in the values. The residual stress at the z plane is a tensile stress of 11 ± 41 MPa in the y direction and 21 ± 127 MPa in the z direction. Fig. 7 shows the damage mode after indentation with a load of 2 N at the x plane. The damaged area of the regions near to the electrode is smaller than that of the far regions, showing the asymmetric damage mode in the near regions to the electrode. Fig. 7 shows that the thermal stress can affect the internal stresses

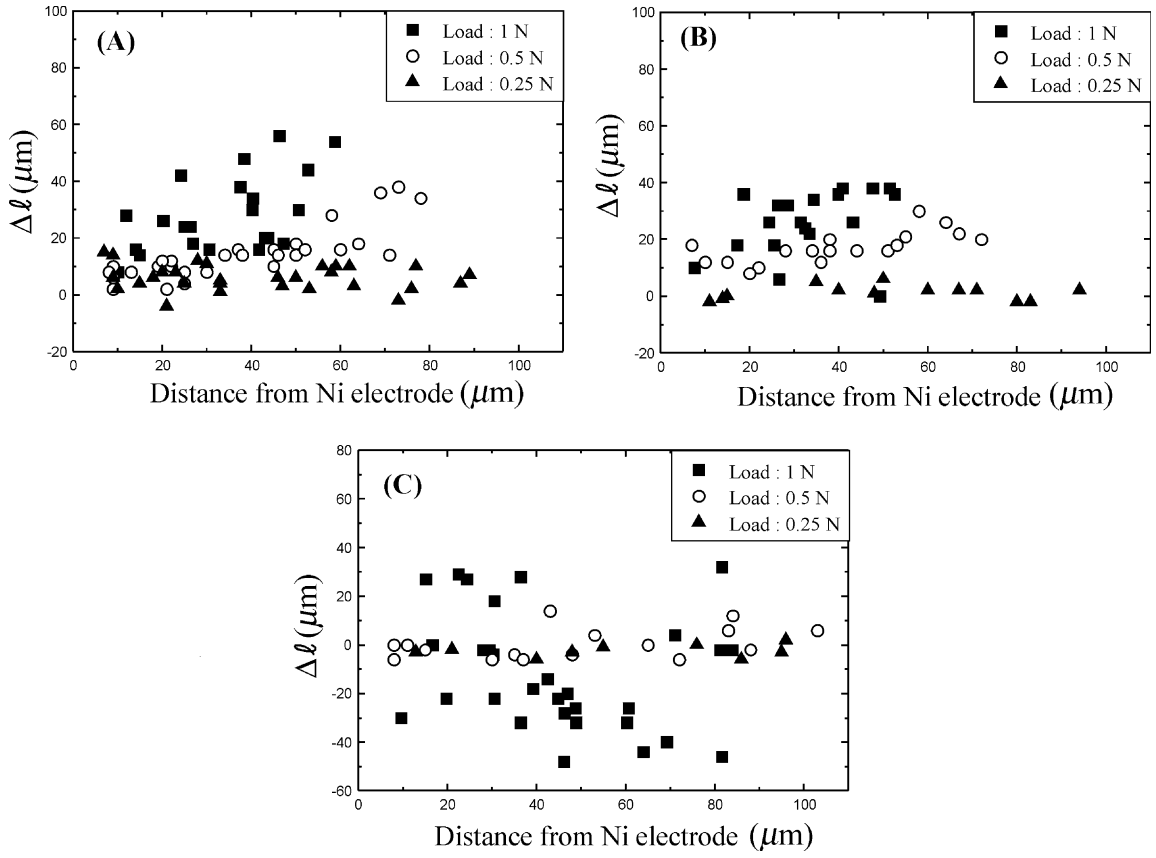

Fig. 3. Difference between crack lengths created with indentation load $P = 0.25$, 0.5, and 1 N: (A) x plane, (B) y plane, and (C) z plane.

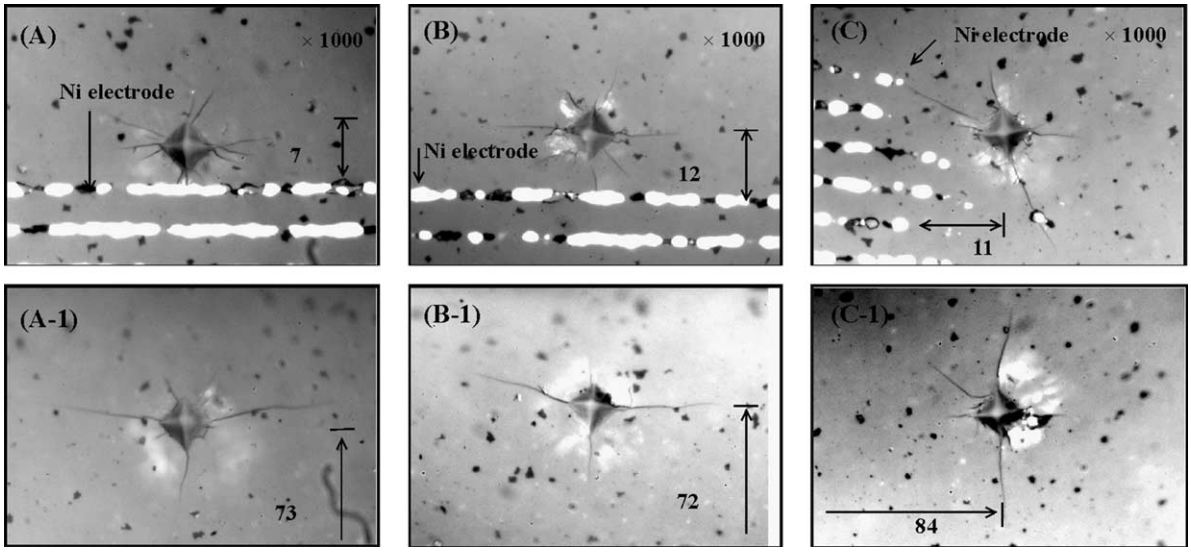

Fig. 4. Micrographs of crack propagation with distance from electrode: A, B, and C series are shown micrographs at x, y, and z planes, respectively.

and mechanical properties within a definite distance from the electrode.

The internal stresses in MLCCs can be originated from the mismatch of material constants between the dielectric and electrode layers, and the fabrication process. The MLCCs have to indicate the residual compressive stress in the margins, based on the theoretical equation, because the thermal expansion coefficient of the dielectric material ($BaTiO_3$) is smaller than that of the electrode (Ni) in $BaTiO_3$ based Ni–MLCCs. The internal stress calculated with the equation is a compressive stress of -274 ± 97 MPa. However, the internal stresses measured in this study—the stresses in the y direction of x plane and in the x direction at y and z

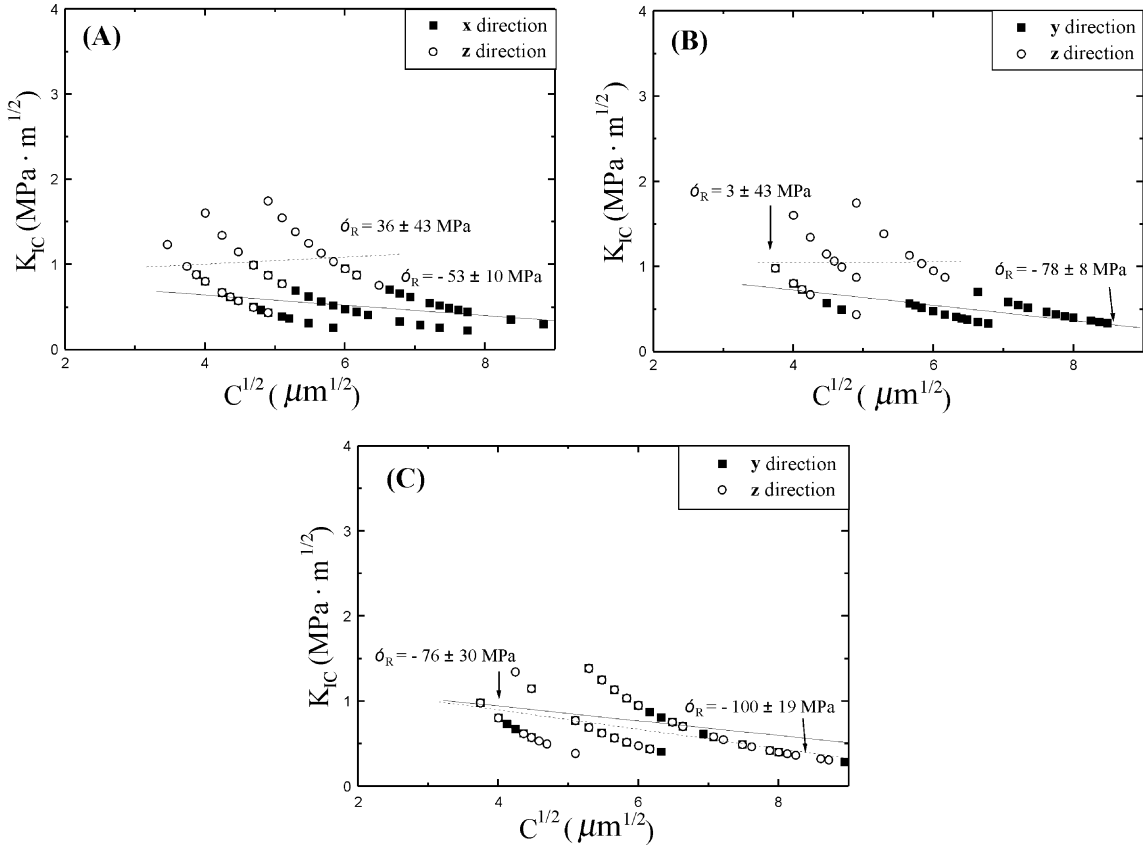

Fig. 5. Residual stresses induced on MLCCs as a function of direction to electrode: (A) *x* plane, (B) *y* plane, and (C) *z* plane.

planes are not measured in this study—are tensile and compressive, depending on the direction with respect to the lamination. The measured compressive stress is smaller than the calculated one. This means that the internal stress derived from the extrinsic stress component (due to the microstructural defects introduced by laminating, burnout and sintering processes) is tensile. Therefore, the extrinsic stress component is much severer than the intrinsic stress component, if the additional stresses generated in MLCCs during the end-termination and soldering processes have to be considered. From this study, it can be postulated that if MLCCs is allowed for the end-termination and soldering processes, a cracking in the margins—especially edge-corner regions—will be created first.

The internal stresses in MLCCs are dependent on the plane and direction, even though the *z* plane does not show the dependence of the direction. The stress unbalance with the direction at the *x* and *y* planes will lead to the different Weibull parameters as reported by Franken and Maier.[4] As yet, it is not clear how the amount of the residual stresses behaves between the dielectric and electrode layers, and/or between the surface of MLCCs and the external electrode of terminating and soldering during the poster processes.

4. Conclusions

The internal stresses in MLCCs have been investigated as functions of the distance from and the direction with respect to the electrode. The hardness in the margins is constant to a distance of ≈70 μm at the *x* plane, ≈45 μm at the *y* plane, and ≈90 μm at the *z* plane, showing the range of 10±1.6, 9.7±1.2, 11±1.2 GPa, respectively, and modestly decreases above that distance. The internal stresses in three planes are compressive and tensile, depending on the plane and the direction to the electrode: a compressive stress of −53±10 MPa in the *x* direction at the *x* plane, of −78±8 MPa in the *y* direction at the *y* plane, and of −76±30 and −100±19 MPa in the *y* and *z* directions at the *z* plane, respectively; a tensile stress of 36±43 and 3±43 MPa in the *z* direction at the *x* and *y* planes, respectively. The internal stress at the *z* plane is not affected by the direction. The extrinsic stress induced by the laminating, burnout, sintering processes is tensile, which is much severer than the intrinsic stress by the material constants, because the internal stresses can be enhanced by processes such as the end-termination and soldering processes. The internal stresses of MLCCs are dependent on the plane with the lamination and the

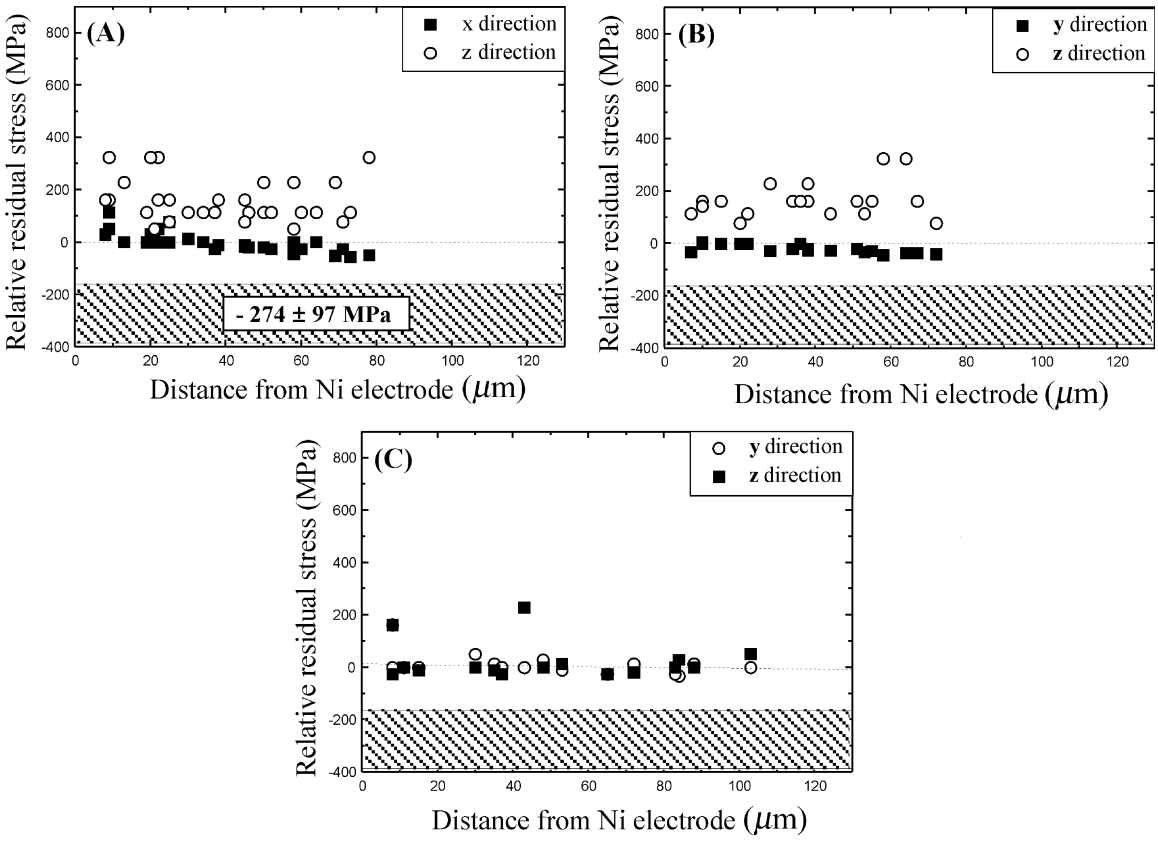

Fig. 6. Relative residual stresses versus distance from electrode as a function of direction to electrode with indentation load $P = 0.5$ N, including thermal stress contribution: (A) x plane, (B) y plane, and (C) z plane.

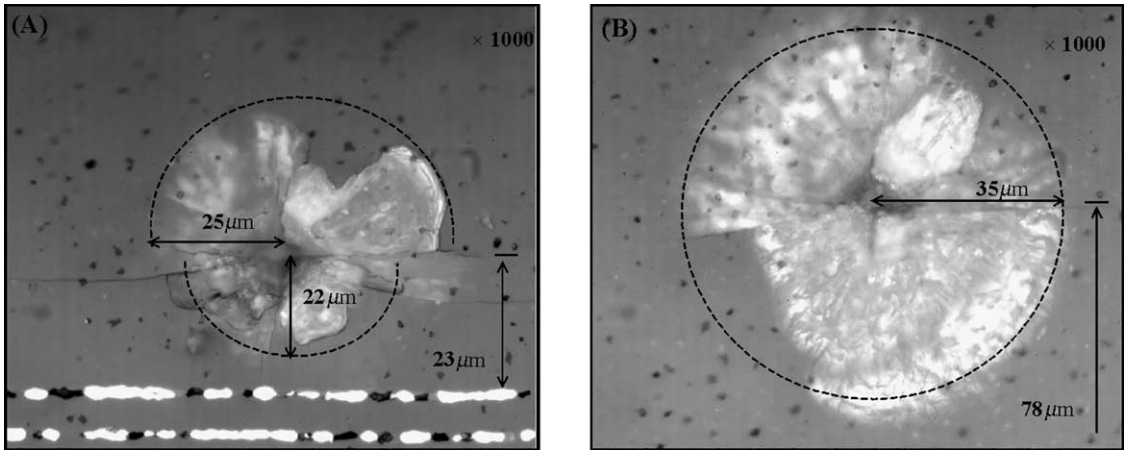

Fig. 7. Micrographs of damage mode after indentation with load $P = 2$ N: (A) 23 μm and (B) 78 μm from electrode.

direction to the electrode, especially in the x and y planes parallel to the electrode.

Acknowledgements

This work has been financially supported by the Korea Institute S & T Evaluation and Planning (KISTEP) through the National Research Laboratory (NRL) in the program year of 2001.

References

1. Cai, H., Gui, Z. and Li, L., Low-sintering composite multilayer ceramic capacitors with X7R specification. *Mater. Sci. Eng.*, 2001, **B83**, 137–141.

2. Prymak, J., *Ceramic Capacitors*. PCIM, September, 1997, pp. 76–80.
3. de With, G., Structural integrity of ceramic multilayer capacitor materials and ceramic multilayer capacitors. *J. Eur. Ceram. Soc.*, 1993, **12**, 323–336.
4. Franken, K. and Maier, H. R., Weibull analysis of soldered MLC under bending load stress. *J. Eur. Ceram. Soc.*, 1999, **19**, 1307–1310.
5. Wereszczak, A. A., Breder, K., Ferber, M. K., Bridge, R. J., Riester, L. and Kirkland, T. P., Failure probability prediction of dielectric ceramics in multilayer capacitors. In *Proceeding of the International Symposium on Multilayer Ceramic Division*, Transactions of the AcerS, 100th Annual Meeting and Exhibition of the American Ceramic Society, Cincinnati, OH, 1998.
6. James, M. R. and Cohen, J. B., *The Measurement of Residual Stresses by X-ray Diffraction Techniques*. Treatise on Materials Science and Technology, Vol. 19. Academic Press, New York, 1980.
7. Dölle, H., The influence of multiaxial stress states, stress gradients and elastic anisotropy on the evaluation of residual stresses by X-rays. *J. Appl. Cryst*, 1979, **12**, 489–501.
8. Bergenthal, J., Mechanical strength properties of multi-layer ceramic chip capacitors. In *11th Capacitor and Resistor Technology Symposium (CARTS)*, 1991.
9. Koripella, C. R., Mechanical behavior of ceramic capacitors. *IEEE Trans. Comp. Hybrids and Manufact. Technol*, 1991, **14**(4), 718–724.
10. de With, G. and Sweegers, N., The effect of erosional wear on strength and residual stress during shaping of ceramic multilayer capacitors. *Wear*, 1995, **188**, 142–149.
11. Marshall, D. B. and Lawn, B. R., An indentation technique for measuring stresses in tempered glass surfaces. *J. Am. Ceram. Soc.*, 1976, **60**, 86–87.
12. Marshall, D. B. and Lawn, B. R., Residual stress effects in sharp-contact cracking. I. Indentation fracture mechanics. *J. Mater. Sci.*, 1979, **14**(8), 2001–2012.
13. Suresh, S. and Giannakopoulos, A. E., A new method for estimating residual stresses by instrumented sharp indentation. *Acta Mater.*, 1998, **46**(16), 5744–5797.
14. Suresh, S. and Giannakopoulos, A. E., *Method and Apparatus for Determining Preexisting Stresses Based on Indentation or Other Mechanical Probing of the Material*. US Patent application, filed May 1998.
15. Karlsson, L., Hultman, L. and Sundgren, J. E., Influence of residual stresses on the mechanical properties of TiC_xN_{1-x} ($x=0$, 0.15, 0.45) thin films deposites by arc evaporation. *Thin Solid Films*, 2000, **371**, 167–177.
16. Almer, J., Odén, M. and Håkansson, G., Microstructure, stress and mechanical properties of arc-evaporated Cr-C-N coating. *Thin Solid Films*, 2001, **385**, 190–197.
17. Rawal, B., Ladew, R. and Garcia, R., Factors Responsible for thermal shock behavior of chip capacitors. In *Proceedings of the 37th Electronic Components Conferences*, Boston, MA, 1987, pp. 145–156.
18. White, G. S., Nguyen, C. and Rawal, B., Young's modulus and thermal diffusivity measurements of barium titanate based dielectric ceramics. In *Proceedings of Nondestructive Testing of High Performance Ceramics*, 1987, pp. 371–379.
19. Lide, D. R., *CRC Handbook of Chemistry and Physics*, 81st edn. CRC Press, Boca Raton, London, New York, Washington, DC, 2000.